Chapter 4

Convection

We learned in Chapters 2 and 3 that terrestrial radiation emanates to space primarily from the upper troposphere, rather than the ground; much of what radiates from the surface is absorbed within the atmosphere. The surface is thus warmed by both direct solar radiation and downwelling terrestrial radiation from the atmosphere. In consequence, in radiative equilibrium, the surface is warmer than the overlying atmosphere. However, it turns out that this state is *unstable* to convective motions which develop, as sketched in Fig.4.1, and transport heat upward from the surface. In the troposphere, therefore, equilibrium is not established solely by radiative processes. In this chapter, we discuss the nature of the convective process and its role in determining the *radiative-convective* balance of the troposphere.

As we are about to explore, the conditions under which convection occurs depend on the characteristics of the fluid; consequently, the theory appropriate in a moist, compressible atmosphere is somewhat more complicated than in an incompressible medium like water. Accordingly, we will discuss convection in a sequence of cases of increasing complexity. After making some general remarks about the nature of convection, we will describe the incompressible case — using a theoretical approach and a laboratory experiment — in Section 4.2. Convection in an unsaturated compressible atmosphere is discussed in Section 4.3; the effects of latent heat consequent on condensation of moisture are addressed in Section 4.5.

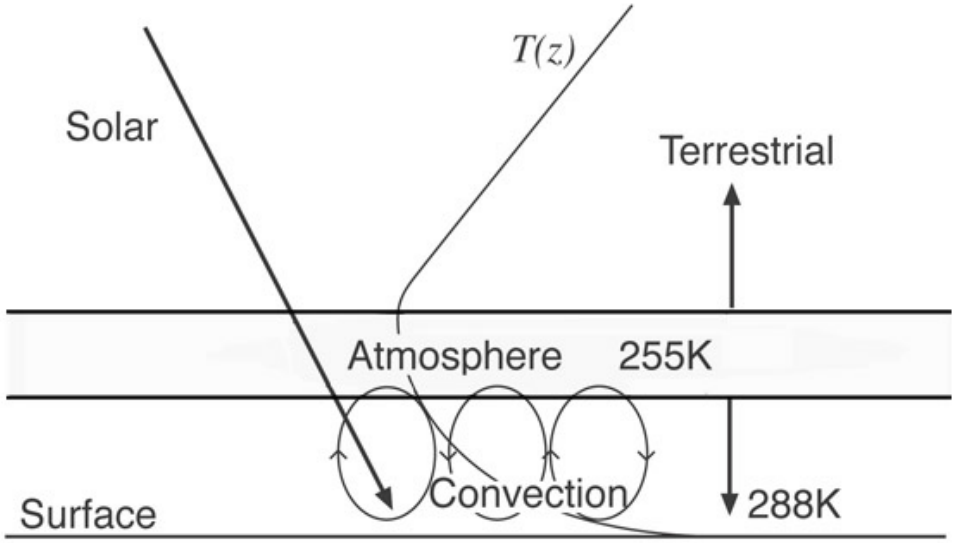

Figure 4.1: Solar radiation warms the earth's surface, triggering convection which carries heat vertically to the emission level from which, because the atmosphere above this level is transparent in the IR, energy can be radiated out to space. The surface temperature of about 288 K, is significantly higher than the temperature at the emission level, 255 K, because the energy flux from the surface must balance not just the incoming solar radiation but also downwelling IR radiation from the atmosphere above. An idealized radiative equilibrium temperature profile, $T(z)$ is superimposed (cf. Fig.2.11).

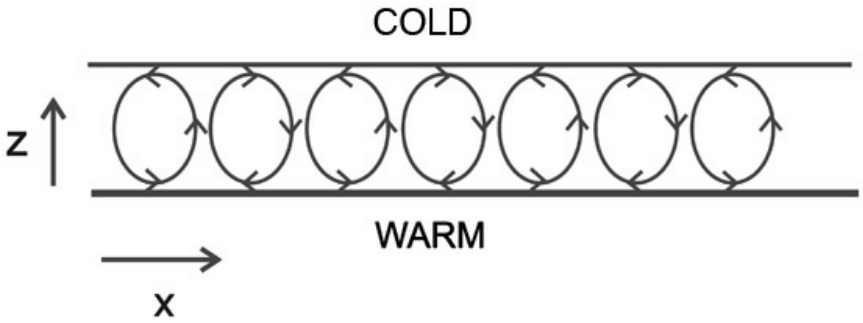

Figure 4.2: Schematic of shallow convection in a fluid such as water triggered by warming from below and/or cooling from above.

4.1 The nature of convection

4.1.1 Convection in a shallow fluid

When a fluid such as water is heated from below (or, in fact, cooled from above), it develops overturning motions. It may seem obvious that this must occur, because the tendency of the heating (or cooling) is to make the fluid top-heavy[1]. Consider the shallow, horizontally infinite, fluid shown in Fig.4.2. Let the heating be applied uniformly at the base; then we may expect the fluid to have a horizontally uniform temperature, so $T = T(z)$ only. This will be top-heavy (warmer, and therefore lighter, fluid below cold, dense fluid above). But as we have seen, gravitational forces can be balanced

[1] John William Strutt — Lord Rayleigh (1842-1919) — set the study of convection on a firm theoretical basis in his seminal studies in the 1900's. In one of his last articles, published in 1916, he attempted to explain what is now known as Rayleigh-Benard Convection. His work remains the starting point for most of the modern theories of convection.

by a vertical pressure gradient in hydrostatic balance with the density field [Eq.(3.3)], in which case any fluid parcel will experience zero net force, even if heavy fluid is above light. Nevertheless, observations and experiments show that convection develops[2], as sketched in the figure. Why? There are two parts to the question:

1. Why do motions develop, when the equilibrium state discussed above has no net forces anywhere?

2. Why are the motions horizontally inhomogeneous when the external forcing (the heating) is horizontally uniform?

The answer is that the motions are not directly forced, but (like many types of motion in the atmosphere and ocean) arise from an *instability* of the fluid in the presence of heating. We therefore begin our discussion of convection by reminding ourselves of the nature of instability.

4.1.2 Instability

For any system that possesses some equilibrium state, instability will arise if, in response to a perturbation, the system tends to drive the perturbation further from the equilibrium state. A simple and familiar example is a ball on a curved surface, as in Fig.4.3.

A ball that is stationary and exactly at a peak (point A, $x = x_A$) is in equilibrium but, of course, this state is unstable. If the ball is displaced a small distance δx from A, it finds itself on a downward slope, and therefore is accelerated further. To be specific, the component of gravitational acceleration along the slope is, for small slope, $-g\, dh/dx$. The slope at $x_A + \delta x$ is, making a Taylor expansion about $x = x_A$ (see Section 13.2.1),

$$\frac{dh}{dx}(x_A + \delta x) \simeq \frac{dh}{dx}(x_A) + \left(\frac{d^2h}{dx^2}\right)_A \delta x = \left(\frac{d^2h}{dx^2}\right)_A \delta x$$

for small δx, since the slope is zero at x_A. Hence the equation of motion for the ball is

$$\frac{d^2}{dt^2}(\delta x) = -g\frac{\partial h}{\partial x} = -g\left(\frac{d^2h}{dx^2}\right)_A \delta x\ . \tag{4.1}$$

[2]We are considering here the stability of a fluid that has no (or, rather, very small) viscosity and diffusivity. Rayleigh noted that convection of a viscous fluid heated from below does not always occur; for example, oatmeal or polenta burns if it is not kept stirred because the high viscosity can prevent convection currents.

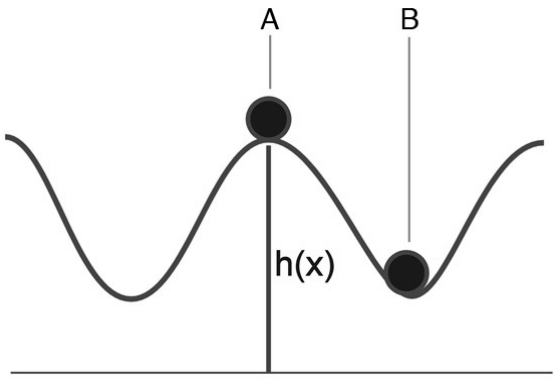

Figure 4.3: Stability and instability of a ball on a curved surface.

This has solutions

$$\delta x(t) = c_1 e^{\sigma_+ t} + c_2 e^{\sigma_- t} \tag{4.2}$$

where c_1, c_2 are constants and

$$\sigma_\pm = \pm\sqrt{-g\left(\frac{d^2h}{dx^2}\right)_A}.$$

At a peak, where dh/dx changes from positive to negative with increasing x, $d^2h/dx^2 < 0$, both roots for σ are real, and the first term in Eq.(4.2), describes an exponentially growing perturbation; the state (of the ball at A in Fig.4.3) is *unstable*. (Exponential growth will occur only for as long as our assumption of a small perturbation is valid and will obviously break down before the ball reaches a valley.) On the other hand, for an equilibrium state in which $d^2h/dx^2 > 0$ (such as the valley at B), the roots for σ are imaginary, Eq.(4.2) yields oscillatory solutions and the state is *stable* — any perturbation will simply produce an oscillation as the ball rolls back and forth across the valley.

A consideration of the energetics of our ball is also instructive. Rather than writing down and solving differential equations describing the motion of the ball, as in Eq.(4.1), the stability condition can be deduced by a consideration of the energetics. If we perturb the ball in a valley, it moves up the hill and we have to do work (add energy) to increase the potential energy

of the ball. Hence, in the absence of any external energy source, the ball will return to its position at the bottom of the valley. But if the ball is perturbed on a crest it moves downslope, its potential energy *decreases* and its kinetic energy *increases*. Thus we may deduce that state A in Fig.4.3 is unstable and state B is stable.

As we shall now see, the state of heavy fluid over light is an unstable one; the fluid will overturn and return itself to a stable state of lower potential energy.

4.2 Convection in water (an almost-incompressible fluid)

4.2.1 Buoyancy

Objects that are lighter than water bounce back to the surface when immersed, as has been understood since the time of Archimedes (287-212 BC). But what if the 'object' is a parcel[3] of the fluid itself, as sketched in Fig.4.4? Consider the stability of such a parcel in an incompressible liquid. We will suppose that density depends on temperature and not on pressure. Imagine that the parcel shaded in Fig.4.4 is warmer, and hence less dense, than its surroundings.

If there is no motion then the fluid will be in hydrostatic balance. Since ρ is uniform above, the pressure at A_1, A and A_2 will be the same. But, because there is lighter fluid in the column above B than above either point B_1 or B_2, from Eq.(3.4) we see that the hydrostatic pressure at B will be less than at B_1 and B_2. Since fluid has a tendency to flow from regions of high pressure to low pressure, fluid will begin to move toward the low pressure region at B and tend to equalize the pressure along B_1BB_2; the pressure at B will tend to increase and apply an upward force to the buoyant fluid which will therefore begin to move upwards. Thus the light fluid will rise.

In fact (as we will see in Section 4.4) the acceleration of the parcel of fluid is not g but $g\ \Delta\rho/\rho_P$ where $\Delta\rho = (\rho_P - \rho_E)$, ρ_P is the density of the parcel and ρ_E is the density of the environment. It is common to speak of the buoyancy, b, of the parcel, defined as

[3] A 'parcel' of fluid is imagined to have a small but finite dimension, to be thermally isolated from the environment and always to be at the same pressure as its immediate environment.

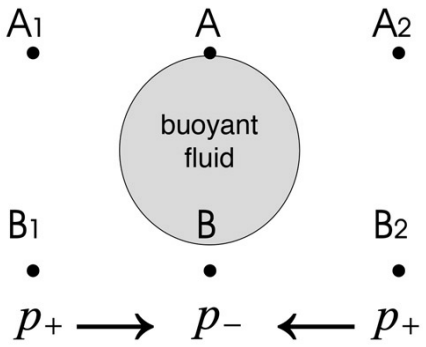

Figure 4.4: A parcel of light, buoyant fluid surrounded by resting, homogeneous, heavier fluid in hydrostatic balance, Eq.(3.3). The fluid above points A_1, A and A_2 has the same density and hence, as can be deduced by consideration of hydrostatic balance, the pressures at the A points are all the same. But the pressure at B is lower than at B_1 or B_2 because the column of fluid above it is lighter. There is thus a pressure gradient force which drives fluid inwards toward B, forcing the light fluid upward.

$$b = -g\frac{(\rho_P - \rho_E)}{\rho_P} \tag{4.3}$$

If $\rho_P < \rho_E$ then the parcel is *positively buoyant* and rises: if $\rho_P > \rho_E$ the parcel is *negatively buoyant* and sinks: if $\rho_P = \rho_E$ the parcel is *neutrally buoyant* and neither sinks or rises.

We will now consider this problem in terms of the stability of a perturbed fluid parcel.

4.2.2 Stability

Suppose we have a horizontally uniform state with temperature $T(z)$ and density $\rho(z)$. T and ρ are assumed here to be related by an equation of state

$$\rho = \rho_{ref}(1 - \alpha[T - T_{ref}]) \tag{4.4}$$

Eq. (4.4) is a good approximation for (fresh) water in typical circumstances, where ρ_{ref} is a constant reference value of the density and α is the coefficient of thermal expansion at $T = T_{ref}$. (A more detailed discussion of the equation

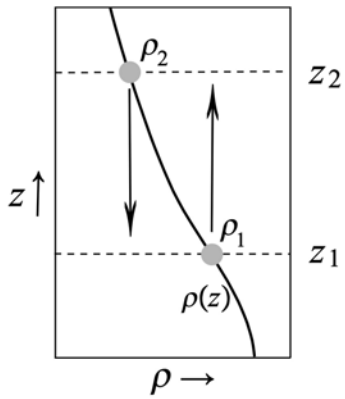

Figure 4.5: We consider a fluid parcel initially located at height z_1 in an environment whose density is $\rho(z)$. It has density $\rho_1 = \rho(z_1)$, the same as its environment at height z_1. It is now displaced adiabatically a small vertical distance to $z_2 = z_1 + \delta z$, where its density is compared to that of the environment.

of state for water will be given in Section 9.1.3). Again we focus attention on a single fluid parcel, initially located at height z_1. It has temperature $T_1 = T(z_1)$ and density $\rho_1 = \rho(z_1)$, the same as its environment; it is therefore *neutrally buoyant*, and thus in equilibrium. Now let us displace this fluid parcel a small vertical distance to $z_2 = z_1 + \delta z$, as shown in Fig.4.5. We need to determine the buoyancy of the parcel when it arrives at height z_2.

Suppose the displacement is done sufficiently rapidly so that the parcel does not lose or gain heat on the way, *i.e.,* the displacement is *adiabatic*. This is a reasonable assumption because the temperature of the parcel can only change by diffusion, which is a slow process compared to typical fluid movements and can be neglected here. Since the parcel is incompressible, it will not contract nor expand, and thus it will do no work on its surroundings; its internal energy and hence its temperature T will be conserved. Therefore the temperature of the perturbed parcel at z_2 will still be T_1, and its density will still be $\rho_P = \rho_1$. The environment, however, has density

$$\rho_E = \rho(z_2) \simeq \rho_1 + \left(\frac{d\rho}{dz}\right)_E \delta z \ ,$$

where $(d\rho/dz)_E$ is the environmental density gradient. The buoyancy of the parcel just depends on the difference between its density and that of its

environment; using Eq.(4.3), we find that

$$b = \frac{g}{\rho_1}\left(\frac{d\rho}{dz}\right)_E \delta z \ .$$

The parcel will therefore be

$$\left.\begin{array}{c}\text{positively}\\ \text{neutrally}\\ \text{negatively}\end{array}\right\} \text{ buoyant if } \left(\frac{d\rho}{dz}\right)_E \left\{\begin{array}{l} > 0 \\ = 0 \\ < 0 \end{array}\right. \ . \tag{4.5}$$

If the parcel is positively buoyant (the situation sketched in Fig.4.4), it will keep on rising at an accelerating rate. Therefore an incompressible liquid is **unstable if density increases with height** (in the absence of viscous and diffusive effects). This is the familiar 'top-heavy' condition. It is this instability that leads to the convective motions discussed above. Using Eq.(4.4) the stability condition can also be expressed in terms of temperature as:

$$\left.\begin{array}{c}\text{unstable}\\ \text{neutral}\\ \text{stable}\end{array}\right\} \text{ if } \left(\frac{dT}{dz}\right)_E \left\{\begin{array}{l} < 0 \\ = 0 \\ > 0 \end{array}\right. \ . \tag{4.6}$$

Note that Eq.(4.6) is appropriate for an incompressible fluid whose density depends only on temperature.

4.2.3 Energetics

Consider now our problem from yet another angle, in terms of energy conversion. We know that if the potential energy of a parcel can be reduced, just like the ball on the top of a hill in Fig.4.3, the lost potential energy will be converted into kinetic energy of the parcel's motion. Unlike the case of the ball on the hill, however, when dealing with fluids we cannot discuss the potential energy of a single parcel in isolation, since any movement of the parcel requires rearrangement of the surrounding fluid; rather, we must consider the potential energy difference between two realizable states of the fluid. In the present case, the simplest way to do so is to consider the potential energy consequences when two parcels are interchanged.

Consider, then, two parcels of incompressible fluid of equal volume at differing heights, z_1 and z_2 as sketched in Fig.4.5. They have the same density as their respective environments. Because the parcels are incompressible they

do not expand or contract as p changes and so do not do work on, nor have work done on them by, the environment. This greatly simplifies consideration of energetics. The potential energy of the initial state is:

$$PE_{initial} = g\left(\rho_1 z_1 + \rho_2 z_2\right).$$

Now interchange the parcels. The potential energy of the final state, after swapping, is

$$PE_{final} = g\left(\rho_1 z_2 + \rho_2 z_1\right).$$

The change in potential energy, ΔPE, is therefore given by:

$$\begin{aligned} \Delta PE &= PE_{final} - PE_{initial} = -g\left(\rho_2 - \rho_1\right)\left(z_2 - z_1\right) \\ &\simeq -g\left(\frac{d\rho}{dz}\right)_E \left(z_2 - z_1\right)^2 \end{aligned} \tag{4.7}$$

if $z_2 - z_1$ is small, where $\left(d\rho/dz\right)_E = \frac{(\rho_2 - \rho_1)}{(z_2 - z_1)}$ is the mean density gradient of the environmental state. Note that the factor $g\left(z_2 - z_1\right)^2$ is always positive and so the sign of ΔPE depends on that of $\left(d\rho/dz\right)_E$. Hence, if $\left(d\rho/dz\right)_E > 0$, rearrangement leads to a decrease in ΔPE and thus to the growth of the kinetic energy of the parcels, *i.e.* a disturbance is able to grow, and the system will be unstable. But if $\left(d\rho/dz\right)_E < 0$ then $\Delta PE > 0$,and potential energy cannot be released by exchanging parcels. So we again arrive at the stability criterion, Eq.(4.6). This energetic approach is simple but very powerful. It should be emphasized, however, that we have only demonstrated the possibility of instability. To show that instability is a fact, one must carry out a stability analysis analogous to that carried out in Section 4.1.2 for the ball on the curved surface (a simple example is given in Section 4.4) in which the details of the perturbation are worked out. However, whenever energetic considerations point to the possibility of convective instability, exact solutions of the governing dynamical equations almost invariably show that instability is a fact, provided diffusion and viscosity are sufficiently weak.

4.2.4 GFD Lab II: Convection

We can study convection in the laboratory using the apparatus shown in Fig.4.6. A heating pad at the base of the tank triggers convection in a fluid

that is initially stratified by temperature. Convection carries heat from the heating pad into the body of the fluid, distributing it over the convection layer much like convection carries heat away from the Earth's surface.

Thermals can be seen to rise from the heating pad, entraining fluid as they rise. Parcels overshoot the level at which they become neutrally buoyant and brush the stratified layer above, generating gravity waves on the inversion (see Fig.4.7 and Section 4.4) before sinking back into the convecting layer beneath. Successive thermals rise higher as the layer deepens. The net effect of the convection is to erode the vertical stratification, returning the fluid to a state of neutral stability — in this case a state in which the temperature of the convecting layer is close to uniform, as sketched in the schematic on the right of Fig.4.6.

Fig.4.8 shows timeseries of T measured by thermometers at various heights above the heating pad (see legend for details). Initially, there is a temperature difference of some 18 °C from top to bottom. After the heating pad is switched on, T increases with time, first for the lowermost thermometer but subsequently, as the convecting layer deepens, for thermometers at each successive height as they begin to measure the temperature of the convecting layer. Note that by the end of the experiment T is rising simultaneously at all heights within the convection layer. We see, then, that the convection layer is well mixed, *i.e.*, of essentially of uniform temperature. Closer inspection of the $T(t)$ curves reveals fluctuations of order $\pm$ 0.1 °C associated with individual convective events within the fluid. Note also that T increases at a rate that is less than linear (this is the subject of Q.3 at the end of this Chapter).

Law of vertical heat transport

We can make use of the energetic considerations discussed in Section 4.2.3 to develop a simple 'law of vertical heat transport' for the convection in our tank which turns out to be a useful model of heat transport in cumulus convection. In order to quantify the transport of heat (or of any other fluid property) we need to define its *flux*. Since the quantity of interest here is the vertical flux, consider fluid moving across a horizontal plane with velocity w; the volume of fluid crossing unit area of the plane during a small time interval δt is just $w\ \delta t$. The heat content of the fluid per unit volume is $\rho c_p T$, where c_p is the specific heat of water; accordingly, the heat flux — the amount of heat

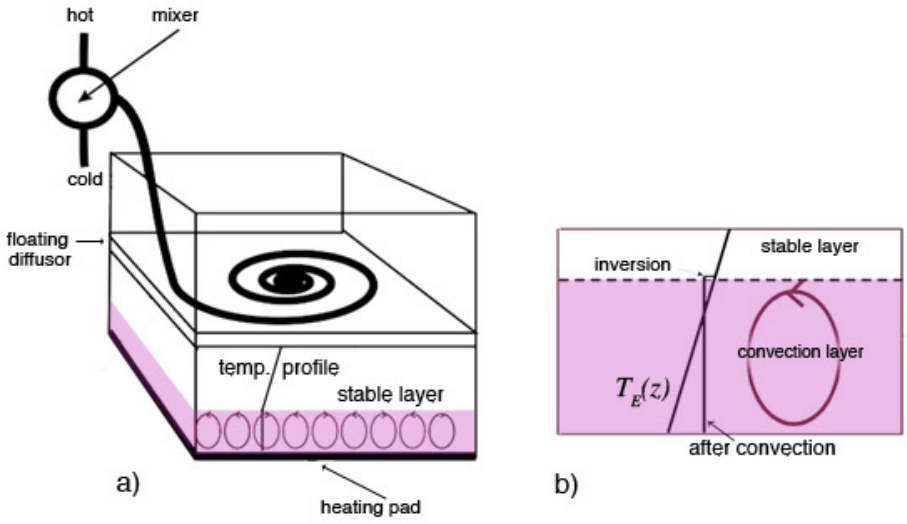

Figure 4.6: (a) A sketch of the laboratory apparatus used to study convection. A stable stratification is set up in a 50 cm×50 cm×50 cm tank by slowly filling it up with water whose temperature is slowly increased with time. This is done using 1) a mixer which mixes hot and cold water together and 2) a diffuser which floats on the top of the rising water and ensures that the warming water floats on the top without generating turbulence. Using the hot and cold water supply we can achieve a temperature difference of 20°C over the depth of the tank. The temperature profile is measured and recorded using thermometers attached to the side of the tank. Heating at the base is supplied by a heating pad. The motion of the fluid is made visible by sprinkling a very small amount of potassium permanganate evenly over the base of the tank (which turns the water pink) after the stable stratification has been set up and just prior to turning on the heating pad. (b) Schematic of evolving convective boundary layer heated from below. The initial linear temperature profile is T_E. The convection layer is mixed by convection to a uniform temperature. Fluid parcels overshoot into the stable stratification above, creating the inversion evident in Fig. 4.7. Both the temperature of the convection layer and its depth slowly increase with time.

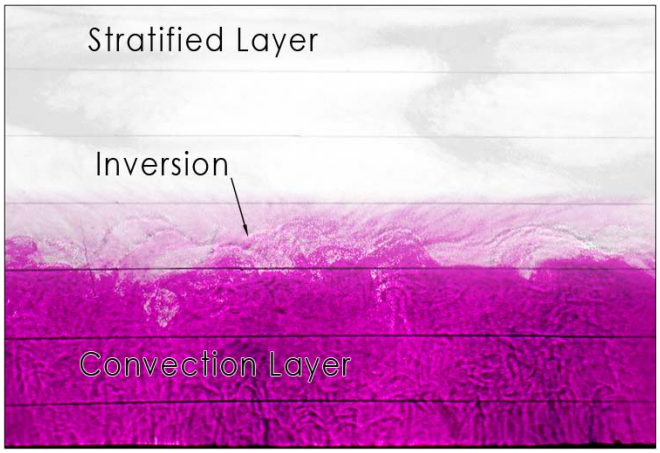

Figure 4.7: A snapshot of the convecting boundary layer in the laboratory exprriment. Note the undulations on the inversion caused by convection overshooting the well mixed layer below into the stratified layer above.

transported across unit volume per unit time — is

$$\mathcal{H} = \rho c_p w T \ . \tag{4.8}$$

In a convecting fluid, this quantity will fluctuate rapidly, and so it will be appropriate to average the flux over the horizontal plane, and in time, over many convective events. In our experiment, we can think of half of the fluid at any level moving upward with typical velocity w_c and temperature $T + \Delta T$, and equal amounts of cool fluid moving downward with velocity $-w_c$ and temperature T. Then the net flux, averaged horizontally, is just $\frac{1}{2}\rho_{ref} c_p w_c \Delta T$.

Now, we found that the change in potential energy resulting from the interchange of the two small parcels of (incompressible) fluid is given by Eq.(4.7). Let us now assume that the potential energy released in convection (as light fluid rises and dense fluid sinks) is acquired by the kinetic energy (KE) of the convective motion:

$$KE = 3 \times \frac{1}{2}\rho_{ref} w_c^2 = \Delta PE = -g\left(\rho_2 - \rho_1\right)\left(z_2 - z_1\right)$$

where we have assumed that the convective motion is isotropic in the three directions of space with typical speed w_c. Using our equation of state for water, Eq.(4.4), we may simplify this to:

$$w_c^2 \simeq \frac{2}{3}\alpha g \Delta z \Delta T \tag{4.9}$$

where ΔT is the difference in temperature between the upwelling and downwelling parcels which are exchanged over a height $\Delta z = z_2 - z_1$. Using Eq.(4.9) in Eq.(4.8) yields the following "law" of vertical heat transfer for the convection in our tank:

$$\mathcal{H} = \frac{1}{2}\rho_{ref} c_p w \Delta T \simeq \frac{1}{2}\rho_{ref} c_p \left(\frac{2}{3}\alpha g \Delta z\right)^{\frac{1}{2}} \Delta T^{\frac{3}{2}} \ . \tag{4.10}$$

In the convection experiment shown in Fig.4.7, the heating pad supplied energy at around $\mathcal{H} = 4000 W\,\mathrm{m}^{-2}$. If the convection penetrates over a vertical scale $\Delta z = 0.2\,\mathrm{m}$, then Eq.(4.10) implies $\Delta T \simeq 0.1\,\mathrm{K}$ if $\alpha = 2 \times 10^{-4}\,\mathrm{K}^{-1}$ and $c_p = 4000\,\mathrm{J\,kg}^{-1}\,\mathrm{K}^{-1}$. Eq.(4.9) then implies a parcel speed of $\simeq 0.5\,\mathrm{cm\ s}^{-1}$. This is not untypical of what is observed in the laboratory experiment.

Thus, convection transfers heat vertically away from the pad. Even though the convection layer is very well mixed, with small temperature fluctuations (as can be seen in the $T(t)$ observations in Fig.4.8) the motions are sufficiently vigorous to accomplish the required transfer.

4.3 Dry convection in a compressible atmosphere

Before we can apply the foregoing ideas to atmospheric convection we must take into account the fact that the atmosphere is a compressible fluid in which $\rho = \rho(p, T)$; specifically, since the atmosphere closely obeys the perfect gas law, $\rho = p/RT$. For now, we will assume a dry atmosphere, deferring consideration of the effects of moisture until Section 4.5. The parcel and environmental pressure, temperature and density at $z = z_1$ in Fig.4.5 are $p_1 = p(z_1)$, $T_1 = T(z_1)$, and $\rho_1 = p_1/RT_1$. The real difference from the incompressible case comes when we consider the adiabatic displacement of the parcel to z_2. As the parcel rises, it moves into an environment of lower pressure. The parcel will adjust to this pressure; in doing so it will expand, doing work on its surroundings, and thus cool. So the *parcel temperature is not conserved* during displacement, even if that displacement occurs adiabatically. In order to compute the buoyancy of the parcel in Fig.4.5 when it arrives at z_2, we need to determine what happens to its temperature.

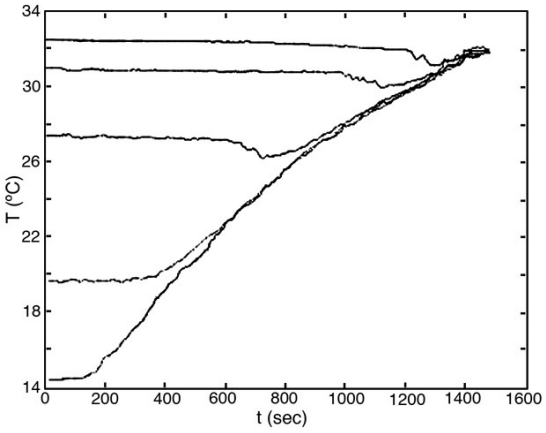

Figure 4.8: Temperature timeseries measured by 5 thermometers spanning the depth of the fluid at equal intervals. The lowest thermometer is close to the heating pad. We see that the ambient fluid initally has a roughly constant stratification, somewhat higher near the top than in the body of the fluid. The heating pad was switched on at $t = 150\,\mathrm{s}$. Note how all the readings converge onto one line as the well mixed convection layer deepens over time.

4.3.1 The adiabatic lapse rate (in unsaturated air)

Consider a parcel of ideal gas of unit mass with a volume V, so that $\rho V = 1$. If an amount of heat, δQ, is exchanged by the parcel with its surroundings then applying the first law of thermodynamics $\delta Q = dU + dW$, where dU is the change in energy and dW is the change in external work done[4], gives us

$$\delta Q = c_v dT + p dV \ , \tag{4.11}$$

where $c_v dT$ is the change in internal energy due to a change in parcel temperature of dT and pdV is the work done by the parcel on its surroundings by expanding an amount dV. Here c_v is the specific heat at constant volume.

Our goal now is to rearrange Eq.(4.11) to express it in terms of dT and dp so that we can deduce how dT depends on dp. To that end we note that, because $\rho V = 1$,

$$dV = d\left(\frac{1}{\rho}\right) = -\frac{1}{\rho^2} d\rho$$

Thus

$$pdV = -\frac{p}{\rho^2} d\rho \ .$$

Repeated use of $p = \rho RT$ yields

$$dp = RT \ d\rho + \rho R \ dT \ ,$$

and

$$p \ dV = -\frac{p}{\rho^2} d\rho = -\frac{p}{\rho^2 RT} dp + \frac{p}{\rho T} dT = -\frac{dp}{\rho} + R \ dT \ .$$

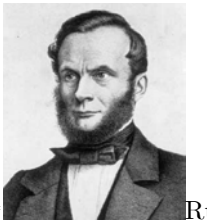

[4] Rudolf Clausius (1822-1888) the Polish physicist, brought the science of thermodynamics into existence. He was the first to precisely formulate the laws of thermodynamics stating that the energy of the universe is constant and that its entropy tends to a maximum. The expression $\delta Q = dU + dW$ is due to Clausius.

The first law, Eq.(4.11) can then be written:

$$\begin{aligned} \delta Q &= (R + c_v)\, dT - \frac{dp}{\rho} \\ &= c_p\, dT - \frac{dp}{\rho}\,, \end{aligned} \tag{4.12}$$

where $c_p = R + c_v$ is the specific heat at constant pressure.

For adiabatic motions, $\delta Q = 0$, whence

$$c_p\, dT = \frac{dp}{\rho}\,. \tag{4.13}$$

Now if the environment is in hydrostatic balance then, from Eq.(3.3), $dp = -g\rho_E\, dz$, where ρ_E is the density of the environment (since the parcel and environmental pressures must be locally equal). Before being perturbed, the parcel's density was equal to that of the environment. If the displacement of the parcel is sufficiently small, its density is still almost equal to that of the environment, $\rho \simeq \rho_E$, and so, under adiabatic displacement, the parcel's temperature will change according to

$$\frac{dT}{dz} = -\frac{g}{c_p} = -\Gamma_d, \tag{4.14}$$

where Γ_d is known as the *dry adiabatic lapse rate*, the rate at which the parcel's temperature decreases with height under adiabatic displacement. Given $c_p = 1005$ J kg^{-1}K^{-1} (Table 1.4), we find $\Gamma_d \simeq 10\,\mathrm{K\ km^{-1}}$.

In order to determine whether or not the parcel experiences a restoring force on being displaced from z_1 to z_2 in Fig.4.5, we must compare its density to that of the environment. At z_2, the environment has pressure p_2, temperature $T_2 \simeq T_1 + (dT/dz)_E\, \delta z$, where $(dT/dz)_E$ is the environmental lapse rate, and density $\rho_2 = p_2/RT_2$. The parcel, on the other hand, has pressure p_2, temperature $T_P = T_1 - \Gamma_d \delta z$, and density $\rho_P = p_2/RT_P$. Therefore the parcel will be positively, neutrally, or negatively buoyant according to whether T_P is greater than, equal to, or less than T_2. Thus our stability condition can be written:

$$\left.\begin{array}{c}\text{UNSTABLE}\\ \text{NEUTRAL}\\ \text{STABLE}\end{array}\right\} \text{ if } \left(\frac{dT}{dz}\right)_E \left\{\begin{array}{l} < -\Gamma_d \\ = -\Gamma_d \\ > -\Gamma_d \end{array}\right. . \tag{4.15}$$

Therefore, a compressible atmosphere is **unstable if temperature decreases with height faster than the adiabatic lapse rate**. This is no

longer a simple "top-heavy" criterion (as we saw in Section 3.3, atmospheric density must decrease with height under all conceivable circumstances). Because of the influence of adiabatic expansion, the temperature must decrease with height more rapidly than the finite rate Γ_d for instability to occur.

The lower tropospheric lapse rate in the tropics is, from Fig.4.9,

$$\left(\frac{dT}{dz}\right)_E \simeq \frac{T(500\text{mbar}) - T(1000\text{mbar})}{Z(500\text{mbar}) - Z(1000\text{mbar})} = \frac{(270 - 295)\ \text{K}}{(5.546 - 0.127)\ \text{km}} \simeq -4.6\,\text{K}\,\text{km}^{-1},$$

or about 50% of the adiabatic value. On the basis of our stability results, we would expect no convection, and thus no convective heat transport. In fact the tropical atmosphere, and indeed the atmosphere has a whole, is almost always *stable* to dry convection; the situation is as sketched in the schematic, Fig.4.10. We will see in Section 4.5 that it is the release of latent heat, when water vapor condenses on expansion and cooling, that leads to convective instability in the troposphere and thus to its ability to transport heat vertically. But, before going on, we will introduce the very important and useful concept of 'potential temperature', a temperature-like variable that *is* conserved in adiabatic motion. This will enable us to simplify the stability condition.

4.3.2 Potential temperature

The nonconservation of T under adiabatic displacement makes T a less-than-ideal measure of atmospheric thermodynamics. However, we can identify a quantity called *potential temperature* which *is* conserved under adiabatic displacement.

Using the perfect gas law Eq.(1.1), our adiabatic statement Eq.(4.13) can be rearranged thus:

$$\begin{aligned} c_p dT &= RT\frac{dp}{p}\,, \\ \frac{dT}{T} &= \frac{R}{c_p}\frac{dp}{p} = \kappa\frac{dp}{p}\,, \end{aligned}$$

where $\kappa = R/c_p = 2/7$ for a perfect diatomic gas like the atmosphere. Thus, noting that $d\ln x = dx/x$, the last equation can be written

$$d\ln T - \kappa d\ln p = 0 \quad \text{or} \quad \frac{T}{p^\kappa} = \text{const.} \tag{4.16}$$

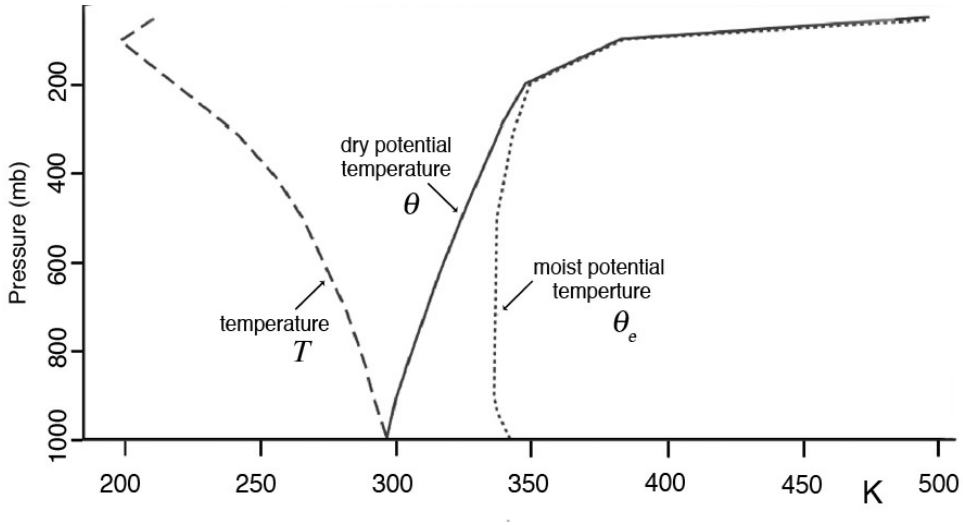

Figure 4.9: Climatological atmospheric temperature T (dashed), potential temperature θ (solid) and equivalent potential temperature θ_e (dotted) as a function of pressure, averaged over the tropical belt $\pm 30°$.

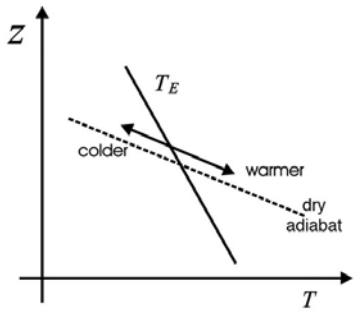

Figure 4.10: The atmosphere is nearly always stable to dry processes. A parcel displaced upwards (downwards) in an adiabatic process moves along a dry adiabat [the dotted line] and cools down (warms up) at a rate that is faster than that of the environment, $\partial T_E/\partial z$. Since the parcel always has the same pressure as the environment it is not only colder (warmer), but also denser (lighter). The parcel therefore experiences a force pulling it back toward its reference height.

Potential temperature, θ, is defined as

$$\theta = T\left(\frac{p_0}{p}\right)^{\kappa} \; ; \tag{4.17}$$

by convention, the constant reference pressure p_0 is taken to be 1000 mbar. It then follows from (4.17), using (4.16), that under adiabatic displacements

$$\frac{d\theta}{\theta} = \frac{dT}{T} - \kappa\frac{dp}{p} = 0 \; .$$

Unlike T, then, θ is conserved in a compressible fluid under (dry) adiabatic conditions.

From its definition, Eq.(4.17), we can see that θ is the temperature a parcel of air would have if it were expanded or compressed adiabatically from its existing p and T to the standard pressure p_0. It allows one, for example, to directly determine how the temperature of an air parcel will change as it is moved around adiabatically: if we know its θ, all we need to know at any instant is its pressure, and then Eq.(4.17) allows us to determine its temperature at that instant. For example, from the climatological profile shown in Fig.4.9, a parcel of air at 300 mbar has $T = 229\,\mathrm{K}$ ($-44\,^\circ\mathrm{C}$) and $\theta = 323\mathrm{K}$; if the parcel were brought down to the ground ($p = p_0$) adiabatically, thus conserving θ, its temperature would be $T = \theta = 323\,\mathrm{K}$ ($50\,^\circ\mathrm{C}$).

We can express the stability of the column to dry adiabatic processes in terms of θ as follows. Let's return to our air parcel in Fig.4.5. At the undisturbed position z_1 it has environmental temperature and pressure, and therefore also environmental potential temperature $\theta_1 = \theta_E(z_1)$, where $\theta_E(z)$ is the environmental profile. Since the parcel preserves θ in adiabatic motion, it still has $\theta = \theta_1$ when displaced to z_2. The parcel pressure is the same as that of its environment and so, from Eq.(4.17), it is warmer (or cooler) than its environment according to whether θ_1 is greater (or lesser) than $\theta_E(z_2)$. Since $\theta_E(z_2) \simeq \theta_E(z_1) + (d\theta/dz)_E\,\delta z = \theta_1 + (d\theta/dz)_E\,\delta z$, the parcel is

$$\left.\begin{array}{c}\text{UNSTABLE}\\ \text{NEUTRAL}\\ \text{STABLE}\end{array}\right\} \text{ if } \left(\frac{d\theta}{dz}\right)_E \left\{\begin{array}{l} < 0\\ = 0\\ > 0\end{array}\right. \; . \tag{4.18}$$

Note that Eq.(4.18) has the same form as Eq.(4.6) for an incompressible fluid, but is now expressed in terms of θ rather than T. So another way

of expressing the instability criterion is that a compressible atmosphere is unstable if **potential temperature decreases with height**.

Fig.4.9 shows climatological T and θ as functions of pressure up to 100 mbar, averaged over the tropical belt. Note that $\frac{d\theta}{dz} > 0$, but that $\frac{dT}{dz} < 0$. As noted earlier, we see that the climatological state of the atmosphere is stable to *dry* convection. However, dry convection is often observed in hot arid regions such as deserts (e.g the Sahara desert or Arizona) where the surface can become very hot and dry. This state of affairs is sketched in Fig.4.11. Air parcels rise from the surface and follow a dry adiabat (conserving potential temperature) until their temperature matches that of the environment, when they will become neutrally buoyant. (In reality, the rising parcels have nonzero momentum, so they may overshoot the level of neutral buoyancy, just as observed in our laboratory convection experiment. Conversely, they may also entrain cooler air from the environment, thus reducing their buoyancy and limiting their upward penetration.) So, in Fig.4.11(left), if the surface temperature is T_1 (or T_2), convection will extend to an altitude z_1 (or z_2). This is the atmospheric, and therefore compressible, analogue of the convection of an incompressible fluid (water) studied in GFD LabII, Section 4.2.4. The analogy becomes even clearer if one views the same process in terms of θ, as sketched in Fig.4.11(right). The convective layer is of uniform θ corresponding to neutral stability, just as observed in the laboratory experiment (*cf.*, Fig.4.6).

4.4 The atmosphere under stable conditions

4.4.1 Gravity waves

The ball perched on the peak in Fig.4.3 is unstable, just like the atmosphere under convectively unstable conditions. We have seen, however, that the atmosphere is mostly stable to dry processes (*i.e.*, $dT/dz > -\Gamma_d$) and so the analogy is with the ball in the valley: when disturbed, a dry air parcel will simply oscillate about its mean position.

In order to analyze this situation, we once again consider the buoyancy forces on a displaced air parcel. Consider Fig.4.12. An air parcel has been displaced upward, adiabatically, a distance Δ from level z_1 to level $z_P = z_1 + \Delta$. The environment has density profile $\rho_E(z)$, and a corresponding pressure field $p_E(z)$ in hydrostatic balance with the density. The parcel's

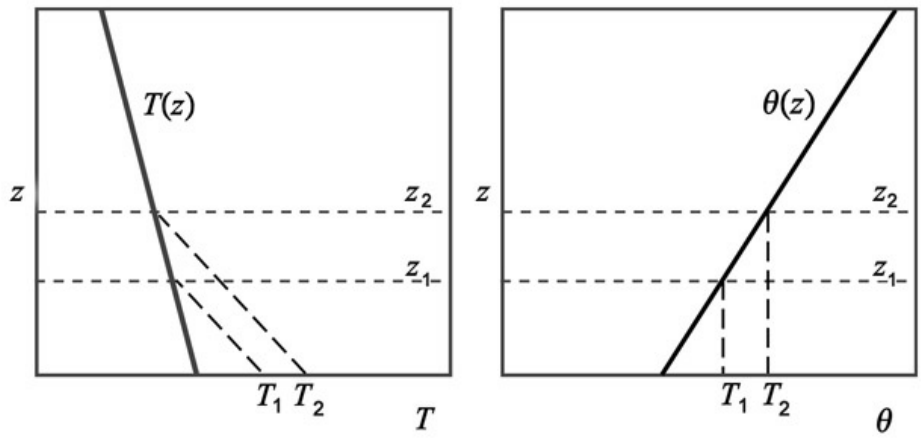

Figure 4.11: Dry convection viewed from the perspective of temperature (left) and potential temperature (right). Air parcels rise from the surface and follow a dry adiabat until their temperature matches that of the environment, when they will become neutrally buoyant. If the surface temperature is T_1 (or T_2), convection will extend to an altitude z_1 (or z_2). The same process viewed in terms of potential temperature is simpler. The stable layer above has $\frac{d\theta}{dz} > 0$; convection returns the overturning layer to a state of uniform θ corresponding to neutral stability, just as observed in the laboratory experiment (cf. the right frame of Fig.4.6). Note that by definition, $\theta = T$ at $p = 1000\text{h}\,\text{Pa}$.

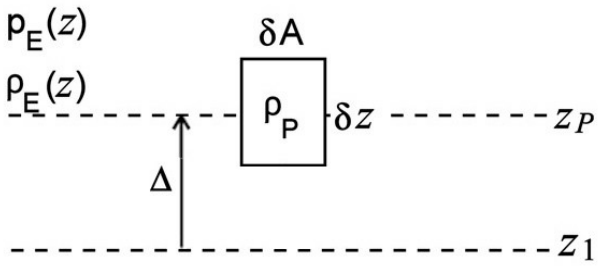

Figure 4.12: A parcel displaced a distance Δ from height z_1 to height z_P. The density of the parcel is ρ_P, and that of the environment, ρ_E.

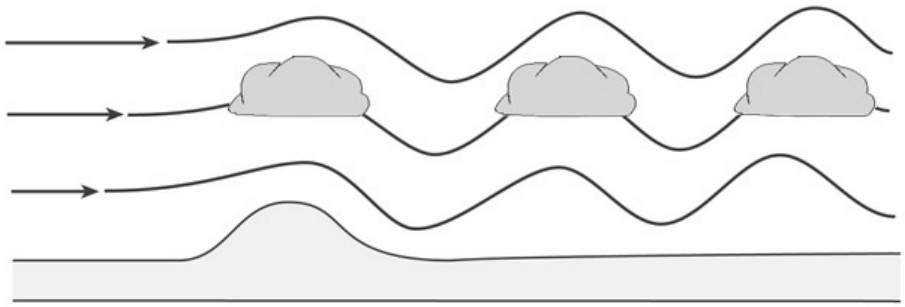

Figure 4.13: A schematic diagram illustrating the formation of mountain waves (also known as lee waves). The presence of the mountain disturbs the air flow and produces a train of downstream waves (cf., the analogous situation of water in a river flowing over a large submerged rock, producing a downstream surface wave train). Directly over the mountain, a distinct cloud type known as lenticular ("lens-like") cloud is frequently produced. Downstream and aloft, cloud bands may mark the parts of the wave train in which air has been uplifted (and thus cooled to saturation).

pressure must equal the environmental pressure; the parcel's density is $\rho_P = p_P/RT_P = p_E(z_P)/RT_P$. We suppose the parcel has height δz, and cross-sectional area δA.

Now, the forces acting on the parcel are (following the arguments and notation given in Section 3.2):

i) gravity, $F_g = -g\ \rho_P\ \delta A \delta z$ (downwards) and

ii) net pressure force $F_T + F_B = -\delta p_E\ \delta A = g\rho_E \delta A \delta z$ (upwards)

where we have used hydrostatic balance. Hence the net force on the parcel is

$$F_g + F_T + F_B = g\,(\rho_E - \rho_P)\,\delta A\ \delta z\ \ .$$

The parcel's mass is $\rho_p \delta z \delta A$, and the equation of motion for the parcel is therefore

$$\rho_P\ \delta z\ \delta A\ \frac{d^2\Delta}{dt^2} = g\,(\rho_E - \rho_P)\,\delta A\ \delta z\ ,$$

i.e.,

$$\frac{d^2\Delta}{dt^2} = -g\left(\frac{\rho_P - \rho_E}{\rho_P}\right). \tag{4.19}$$

Figure 4.14: Looking downwind at a series of lenticular wave clouds in the lee of the Continental Divide of North America. (Photo courtesy of Dale Durran.)

The quantity $b = -g\left(\rho_P - \rho_E\right)/\rho_P$ is, of course, the buoyancy of the parcel as defined in Eq.(4.3): if $\rho_P > \rho_E$ the parcel will be negatively buoyant. Now, because the parcel always has the same pressure as the environment, we may write its buoyancy, using the ideal gas law Eq.(1.1) and the definition of potential temperature, Eq.(4.17), as

$$b = g\frac{\rho_E - \rho_P}{\rho_P} = \frac{g}{T_E}\left(T_P - T_E\right) = \frac{g}{\theta_E}\left(\theta_P - \theta_E\right) \tag{4.20}$$

For small Δ, $\theta_E\left(z+\Delta\right) = \theta_E\left(z_1\right) + \Delta\frac{d\theta_E}{dz}$. Moreover, since the potential temperature of the parcel is conserved, $\theta_P = \theta_E(z_1)$, and so $\theta_P - \theta_E = -\Delta\frac{d\theta_E}{dz}$, enabling Eq.(4.19) to be written:

$$\frac{d^2\Delta}{dt^2} = -\frac{g}{\theta_E}\frac{d\theta_E}{dz}\Delta = -N^2\Delta \tag{4.21}$$

where we define

$$N^2 = \frac{g}{\theta_E}\frac{d\theta_E}{dz} \tag{4.22}$$

Figure 4.15: Atmospheric gravity waves formed in the lee of Jan Mayen island (only 50 km long situated 375 miles north-northeast of Iceland), observed in February 2000. The wind is blowing from the WSW. A volcano — called Beerenberg — forms the north end of the island and rises to a height of over 2 km. Note the similarity between the atmospheric wake and that formed on a water surface by a ship, superimposed on the figure.

which depends only on the vertical variation of θ_E. Note that, under the stable conditions assumed here, $N^2 > 0$, so N is real. Then Eq.(4.21) has *oscillatory* solutions of the form

$$\Delta = \Delta_1 \cos Nt + \Delta_2 \sin Nt \ ,$$

where Δ_1 and Δ_2 are constants set by initial conditions and N, defined by Eq.(4.22), is the frequency of the oscillation. It is for this reason that the quantity N (with units of s^{-1}) is known as the *buoyancy frequency*.

Thus, in the stable case, the restoring force associated with stratification allows the existence of waves, which are known as *internal gravity waves*, and which are in fact analogous to those commonly seen on water surfaces. The latter, known as *surface gravity waves*, owe their existence to the stable,

"bottom heavy", density difference at the water-air interface. Internal gravity waves owe their existence to a continuous, internal, stable stratification.

Under typical tropospheric conditions (see the θ profile in Fig.4.9), we estimate

$$N^2 = \frac{9.81\,\mathrm{m\,s^{-2}}}{300\,\mathrm{K}} \times \frac{340\,\mathrm{K} - 300\,\mathrm{K}}{10^4\,\mathrm{m}} = 1.3 \times 10^{-4}\,\mathrm{s^{-2}},$$

whence internal gravity waves in the atmosphere have a typical period of $2\pi/N \simeq 9\,\mathrm{min}$[5]. Internal gravity waves are ubiquitous in the atmosphere and are continually excited by, *e.g.*, horizontal winds blowing over hills and mountains, and convective plumes buffeting a stable layer above, amongst other things. On occasion, when the air is nearly saturated, they are made visible by the presence of regular bands of clouds in the crest of each wave (but not all visible bands of clouds are produced in this way). These clouds often have a characteristic 'lens' shape, hence the name 'lenticular.' (Fig. 4.14 shows an example.) One can (very roughly) estimate an expected horizontal wavelength for the waves as follows. If each parcel of air oscillates at frequency N but is carried along by the wind at speed u, such that a stationary pattern results, as in Fig.4.15, then the expected wavelength is $2\pi u/N$, around $5 - 10\,\mathrm{km}$ for the N estimated above and a wind of $10 - 20\,\mathrm{m\,s^{-1}}$. Regular cloud features of this type are especially dramatic in the vicinity of mountain ranges (such as the Sierra Nevada and the Continental Divide of North America), as illustrated in Fig.4.13 and shown in the photograph Fig.4.14. Another rather spectacular example of internal gravity waves in the atmosphere is shown in Fig.4.15 and has an uncanny resemblance to the wake left by a ship (superimposed on the figure).

We shall see in Chapter 9 that the interior of the ocean is also stably stratified: internal gravity waves are a ubiquitous feature of the ocean too. Features indicative of such waves have also been observed in the Martian and Jovian atmospheres.

4.4.2 Temperature inversions

In abnormal situations in the troposphere in which T actually increases with height, the atmosphere is very stable: the restoring force on a lifted air parcel

[5] In fact, the frequency given by Eq.(4.22) is an upper limit. We have considered the case in which the parcels of air oscillate exactly vertically. For parcel oscillations at an angle α to the vertical, the frequency is $N\cos\alpha$.

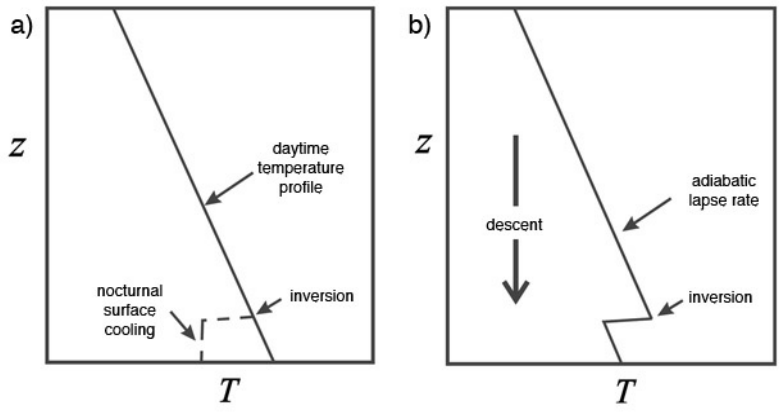

Figure 4.16: (a) Low-level inversions are commonly produced during calm winter nights, as a result of radiative cooling of the surface (b) A trade inversion created by descent and adiabatic warming typical of subtropical regions.

is large and the atmosphere is thus particularly resistive to vertical motion. Such "inversions" can be produced in several ways. Low-level inversions (at altitudes of a few hundred meters) are commonly produced during calm winter nights, as a result of radiative cooling of the surface (see Fig.4.16a).

Note that the inversion may be self-reinforcing: under conditions of slight wind, turbulence carries heat from aloft and limits the cooling of the surface; if an inversion forms, the resistance to vertical motion suppresses the turbulence and allows the surface layer to cool, thus strengthening the inversion. (Fog may then form in the cold surface layer below the inversion.) Apart from its thermal impact, the inversion may trap surface air and thus allow pollutants to build up in the surface layer.

A second type of low-level inversion, common in many subtropical regions of the Earth, is known as the *trade-wind*, or just *trade*, inversion. As we shall see in Chapter 5, air in the subtropics is, on average, descending and thus *warms* adiabatically, according to Eq.(4.14), as it does so. As shown in Fig.4.16b, this can produce a persistent inversion (at altitudes of between 400 m and 2 km, depending on location). Many subtropical cities have pollution problems that are exacerbated by the trade inversion. In some cases, the vertical trapping of air by the inversion can be compounded by horizontal trapping by mountains. Los Angeles and Mexico City (and many other

cities) suffer from this situation (Fig.4.17).

4.5 Moist convection

We have seen that the atmosphere, in most places and at most times, is stable to dry convection. Nevertheless, convection is common in most locations over the globe (more so in some locations than in others, as we will show in Section 4.6.2). There is one very important property of air that we have not yet incorporated into our discussion of convection. Air is *moist*, and if a moist air parcel is lifted it cools adiabatically; if this cooling is enough to saturate the parcel, some water vapor condenses to form cloud. The corresponding latent heat release adds buoyancy to the parcel, thus favoring instability. This kind of convection is called 'moist convection.' In order to derive a stability condition for moist convection we must first discuss how to describe the moisture content of air.

4.5.1 Humidity

The moisture content of air is conveniently expressed in terms of humidity. The **specific humidity**, q, is a measure of the mass of water vapor to the mass of air per unit volume defined thus:

$$q = \frac{\rho_v}{\rho} \,, \tag{4.23}$$

where $\rho = \rho_d + \rho_v$ (Section 1.3.2) is the total mass of air (dry air plus water vapor) per unit volume. Note that in the absence of mixing or of condensation, specific humidity is conserved by a moving air parcel, since the masses of both water and air within the parcel must be separately conserved.

The **saturation specific humidity**, q_*, is the specific humidity at which saturation occurs. Since both water vapor and dry air behave as perfect gases, using Eq.(1.2) to express Eq.(4.23) at saturation, we define q_* thus:

$$q_* = \frac{e_s/R_v T}{p/RT} = \left(\frac{R}{R_v}\right)\frac{e_s}{p} \,. \tag{4.24}$$

where $e_s(T)$ is the saturated partial pressure of water vapor plotted in Fig.1.5. Note that q_* is a function of temperature *and* pressure. In particular, at fixed p it is a strongly increasing function of T.

Figure 4.17: (Top) A satellite image showing dense haze associated with pollution over eastern China. The view looks eastward across the Yellow Sea towards Korea. Provided by the SeaWiFS Project, NASA/Goddard Space Flight Center. (bottom) Temperature inversions in Los Angeles often trap the pollutants from automobile exhaust and other pollution sources near the ground.

Relative humidity, U, is the ratio of the specific humidity to the *saturation specific humidity*, q_*, often expressed as a percentage thus:

$$U = \frac{q}{q_*} \times 100\% \tag{4.25}$$

Now, near the Earth's surface, the moisture content of air is usually fairly close to saturation (*e.g.*, throughout the lower tropical atmosphere, the relative humidity of air is close to 80%, as will be seen in Chapter 5). If such an air parcel is lifted the pressure will decrease and it will cool. From Eq.(4.24), decreasing pressure alone would make q_* increase with altitude. However, the exponential dependence of e_s on T discussed in Chapter 1 overwhelms the pressure dependence and, in consequence, q_* decreases rapidly with altitude. So, as the air parcel is lifted, conserving its q, it does not usually have to rise very far before $q > q_*$. The level at which this occurs is called the *condensation level* z_c (Fig.4.18). At and above z_c, excess vapor will condense so that $q = q_*$. Moreover, since q_* will continue to decrease as the parcel is lifted further, q will decrease correspondingly. Such condensation is visible, *e.g.*, as convective clouds. As the vapor condenses, latent heat release partly offsets the cooling due to adiabatic expansion. Thus we expect the moist parcel to be more buoyant than if it were dry. As illustrated in Fig.4.18, above z_c, the parcel's temperature falls off more slowly (contrast with the dry convection case, Fig.4.11) until neutral buoyancy is reached at z_t, the cloud top. Clearly, the warmer or moister the surface air, the higher the cloud top will be.

Below the condensation level we expect a parcel undergoing convection to follow a dry adiabat. But how does its temperature change in the saturated layer above? It follows a 'saturated adiabat,' as we now describe.

4.5.2 Saturated adiabatic lapse rate

Let us return to the case of a small vertical displacement of an air parcel. If the air is unsaturated, no condensation will occur and so the results of Section 4.3.1 for dry air remain valid. However, if condensation does occur, there will be a release of latent heat in the amount $\delta Q = -L\ dq$ per unit mass of air, where L is the latent heat of condensation and dq is the change in specific humidity q. Thus we must modify Eq.(4.13) to

$$c_p\ dT = \frac{dp}{\rho} - L\ dq \tag{4.26}$$

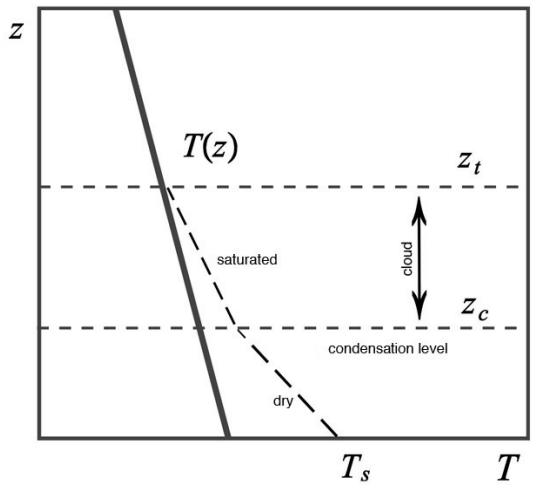

Figure 4.18: The temperature of a moist air parcel lifted in convection from the surface at temperature T_s will follow a dry adiabat until condensation occurs at the condensation level z_c. Above z_c, excess vapor will condense, releasing latent heat and warming the parcel, offsetting its cooling at the dry adiabatic rate due to expansion. Thus a moist parcel cools less rapidly (following a moist adiabat) than a dry one, until neutral buoyancy is reached at z_t, the cloud top. This should be compared to the case of dry convection shown in Fig.4.11.

for an air parcel undergoing moist adiabatic displacement. Note that there is a minus sign here because if $dq < 0$, latent heat is released and the parcel warms. If the environment is in hydrostatic balance, $dp/\rho = -gdz$, and so

$$d\left(c_p T + gz + Lq\right) = 0. \tag{4.27}$$

The term in brackets is known as the *moist static energy* and comprises $c_p T + gz$, the dry static energy and Lq the latent heat content.

If the air parcel is always at saturation, we can replace q by q_* in Eq. (4.26). Now, since $q_* = q_*(p, T)$,

$$dq_* = \frac{\partial q_*}{\partial p} dp + \frac{\partial q_*}{\partial T} dT \ .$$

From (4.24),

$$\frac{\partial q_*}{\partial p} = -\left(\frac{R}{R_v}\right)\frac{e_s}{p^2} = -\frac{q_*}{p}$$

$$\frac{\partial q_*}{\partial T} = \left(\frac{R}{R_v}\right)\frac{1}{p}\frac{de_s}{dT} = \left(\frac{R}{R_v}\right)\frac{\beta e_s}{p} = \beta q_* \ .$$

where we have used Eq.(1.4) to write $de_s/dT = \beta e_s$. Hence Eq.(4.26) gives

$$\left[c_p + L\beta q_*\right] dT = \frac{dp}{\rho}\left[1 + Lq_*\frac{\rho}{p}\right] \ .$$

Writing $dp/\rho = g\ dz$ and rearranging,

$$-\frac{dT}{dz} = \Gamma_s = \Gamma_d\left[\frac{1 + Lq_*/RT}{1 + \beta Lq_*/c_p}\right] \ , \tag{4.28}$$

where Γ_s is known as the *saturated adiabatic lapse rate*[6]. The factor in braces on the right is always less than unity, so the saturated adiabatic lapse rate is less than the dry adiabatic; at high altitudes, however, q_* is small and the difference becomes very small. Since q_* varies with p and T, one cannot ascribe a single number to Γ_s. It has typical tropospheric values ranging between $\Gamma_s \simeq 3$ K km^{-1} in the moist, tropical lower troposphere and $\Gamma_s \simeq \Gamma_d = 10$ K km^{-1} in the upper troposphere. A typical atmospheric temperature profile is sketched, along with dry and saturated adiabats, in Fig.4.19.

The qualitative impact of condensation is straightforward: the release of latent heat makes the air parcel warmer, and therefore more buoyant, and so the atmosphere is *destabilized* by the presence of moisture, *i.e.*, a saturated atmosphere is unstable if

$$\frac{dT}{dz} < -\Gamma_s, \tag{4.29}$$

where $\Gamma_s < \Gamma_d$. The resulting instability is known as *conditional instability*, since it is conditional on the air being saturated. The tropical troposphere is close to neutrality with respect to moist convection, *i.e.*, it has $\partial T/\partial z \simeq -\Gamma_s$ (see section 4.5.3 below).

Lines which show the decrease in T of a parcel of air which is rising/sinking in the atmosphere under saturated adiabatic conditions are called saturated

[6] Γ_s is also known as the *pseudo-adiabatic lapse rate*.

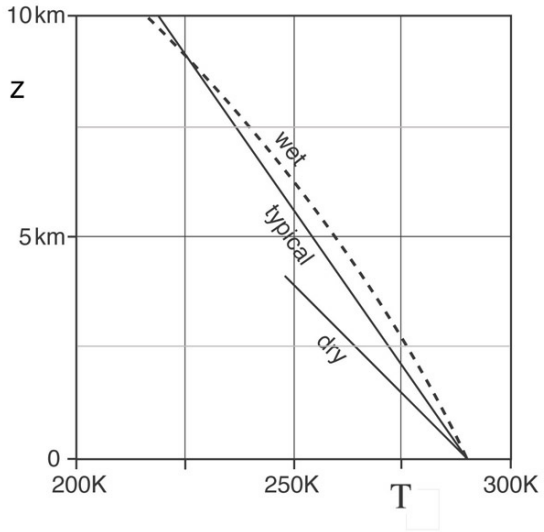

Figure 4.19: A schematic of tropospheric temperature profiles showing the dry adiabat, a typical wet adiabat, and a typical observed profile. Note that the dry adiabatic ascent of a parcel is typically cooler than the surroundings at all levels, whereas the wet adiabat is warmer up to about 10 km. The wet and dry lapse rates are close to one another in the upper troposphere, where the atmosphere is rather dry.

adiabats. As we now describe, we can define a temperature-like quantity which is conserved in moist process and plays an analogous role to that of potential temperature in dry convection.

4.5.3 Equivalent potential temperature

Moist thermodynamics is complicated, but it is relatively straightforward to define a potential temperature that is conserved in moist processes. This quantity, known as equivalent potential temperature, θ_e, tends to be mixed by moist convection, just as dry potential temperature, θ, is mixed in dry convection.

We begin from the first law, Eq.(4.26). Making use of $p = \rho RT$ and $\kappa = R/c_p$, it can be rearranged thus:

$$d \ln T = \kappa d \ln p - \frac{L}{c_p T} dq \ .$$

Now, from the definition of potential temperature, Eq.(4.17), $\ln \theta = \ln T - \kappa \ln p +$ constant, and so this can be written

$$d \ln \theta = -\frac{L}{c_p T} dq \simeq -d \left(\frac{Lq}{c_p T} \right)$$

where we have made the approximation of slipping the factor $L/c_p T$ inside the derivative, on the grounds that the fractional change in temperature is much less than that of specific humidity (this approximation is explored in Q.6 at the end of the Chapter). Then we may conveniently define equivalent potential temperature to be

$$\theta_e = \theta \exp \left(\frac{Lq}{c_p T} \right) \tag{4.30}$$

such that $d\theta_e = 0$ in adiabatic processes. The utility of θ_e is that:

1. It is conserved in both dry and wet adiabatic processes. (In the absence of condensation, q is conserved; hence both θ and θ_e are conserved. If condensation occurs, $q \to q_*(p, T)$; then θ_e is conserved but θ is not.)

2. If the air is dry it reduces to dry potential temperature ($\theta_e \to \theta$ when $q \to 0$).

3. Vertical gradients of θ_e tend to be mixed away by moist convection, just like the T gradient in GFD Lab II.

This last point is vividly illustrated in Fig.4.9 where climatological vertical profiles of T, θ and θ_e are plotted, averaged over the tropical belt $\pm 30^\circ$ (see also Fig.5.9) Note how θ increases with height, indicating that the tropical atmosphere is stable to dry convection. By contrast, the gradient of θ_e is weak, evidence that moist convection effectively returns the tropical atmosphere to a state which is close to neutral with respect to moist processes ($d\theta_e/dp \simeq 0$).

Having derived conditions for convective instability of a moist atmosphere, let us now review the kinds of convection we observe in the atmosphere and their geographical distribution.

4.6 Convection in the atmosphere

We have seen that the atmosphere is normally stable in the absence of condensation. Hence most convection in the atmospheric is moist convection, accompanied by saturation and hence cloud formation. Downwelling air parcels do not become saturated because descending air warms adiabatically. They would therefore become positively buoyant, if it were not for radiative cooling, a process that is much slower than latent heat release in the updrafts; so the descent must be slow. Thus, moist convection comprises narrow, cloudy, vigorous updrafts with larger areas of clear, dry, air slowly descending between.

4.6.1 Types of convection

Convective clouds have two main forms: *cumulus* (Cu) clouds (usually small, 'fair-weather,' and non-precipitating) and *cumulonimbus* (Cb) clouds (usu-

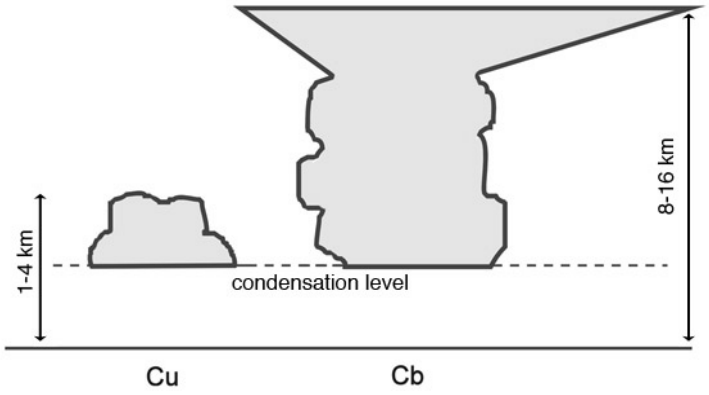

Figure 4.20: Schematic of convective clouds: Cu = cumulus; Cb = cumulonimbus. The condensation level is the level above which $q = q_*$. Cb clouds have a characteristic "anvil" where the cloud top spreads and is sheared out by strong upper level winds.

ally associated with thunderstorms and heavy rain, and perhaps hail)[7].

Modest convection is common and usually shallow (up to just a few km) and capped by Cu clouds (see Figs.4.20 and 4.21). They are typically $1-2\,\mathrm{km}$ tall and towers can be seen to grow this far in about 15 min implying a vertical velocity of around $2\,\mathrm{m\,s^{-1}}$. Typical temperature fluctuations are of order $0.1\,\mathrm{K}$ (see the application of parcel theory below). The sensible heat flux is $\rho c_p \overline{w'T'}$ where the primes denote differences from the time mean, represented by an overbar. Using the above estimates and Table 1.4, we obtain a heat flux of $200\mathrm{W\,m^{-2}}$.

Deep convection is common in the tropics (see Section 4.6.2) and occa-

[7] Luke Howard (1772-1864). An English manufacturing chemist and pharmacist, Howard was also an amateur meteorologist. He wrote one of the first textbooks on weather and developed the basis for our cloud classification system; he is responsible for the cloud nomenclature now in standard use.

Figure 4.21: A well-distributed population of cumulus clouds over the Midwestern United States. Photograph: Russell Windman, May 30, 2002 from an altitude of $35,000\,\mathrm{ft}$.

sional elsewhere. It is manifested by huge Cb clouds, illustrated in Figs.4.20, 4.22, and 4.23, the tops of which may reach the tropopause, and become so cold that the cloud top is sheared off by wind to form an *anvil* made of ice crystals. Vertical motions can reach tens of $\mathrm{m\,s^{-1}}$ with temperature fluctuations of around $1\,\mathrm{K}$. The vertical heat flux associated with individual cumulonimbus clouds is many $\mathrm{kW\ m^{-2}}$. However, they are intermittent both in space and time. They are the primary mechanism of vertical heat transport in the tropics.

Figure 4.22: A mature cumulonimbus (thunderstorm) cloud producing rain and hail on the Great Plains. The hail core is evident in the bright white streaks (center). As the updrafts rise through the cloud and into noticeably warmer air, the top of the cloud spreads out and flattens (top). From the University Corporation for Atmospheric Research.

Figure 4.23: A supercell is a giant Cumulonimbus storm with a deep rotating updraft. Supercells can produce large amounts of hail, torrential rainfall, strong winds and, sometimes, tornadoes. The close-up view of the supercell thunderstorm in the picture shows a bulging dome of clouds extending above the flat, anvil top. This is caused by a very intense updraft which is strong enough to punch through the tropopause and into the stratosphere. At the time of this photograph, baseball-sized hail was falling and a tornado was causing havoc in southern Maryland. Photograph by Steven Maciejewski (April 28, 2002): reported by Kevin Ambrose.

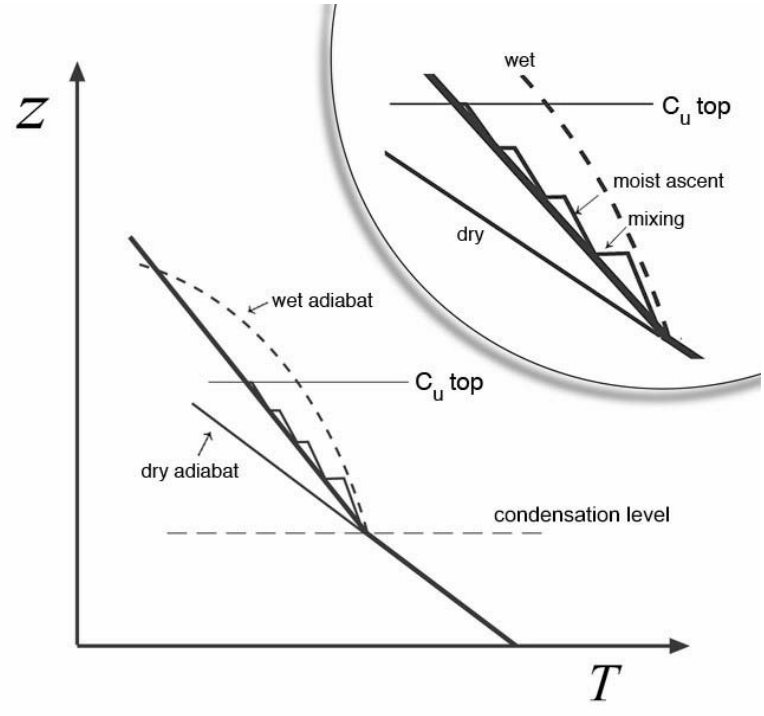

Figure 4.24: In cumulus convection buoyant air parcels ascend along a moist adiabat, but repeatedly mix with ambient fluid, reducing their buoyancy. Cumulus top is expected to occur at the level at which the wet adiabat first runs parallel to the environmental curve, as shown in the inset at top right of figure.

Dynamics of cumulus convection

We have seen that at a certain height, rising moist air parcels become saturated and cloud forms. What happens above cloud base depends on the type of cloud. Cumulus clouds are observed to mix with their surroundings, entraining ambient air. The result is that they rapidly lose their buoyancy. This is illustrated in Fig.4.24 where we sketch air parcels ascending a little along wet adiabats, followed by complete mixing (the short horizontal lines). One consequence evident from the figure is that cumulus top is expected where the wet adiabat first runs parallel to the environmental profile, more or less observed in practice.

A simple model of heat transport in cumulus convection can be con-

structed as follows, in the spirit of the parcel theory developed in Section 4.2.4 to describe convection in our tank of water in GFD Lab II. From Eq.(4.20) we see that the buoyant acceleration of an air parcel is $g\frac{\Delta T}{T}$ where $\Delta T = T_P - T_E$. If the parcel eventually rises by a height Δz, the PE of the system will have decreased by an amount per unit mass of $g\frac{\Delta T}{T}\Delta z$. Equating this to acquired KE, equally distributed between horizontal and vertical components, we find that $\frac{3}{2}w^2 \simeq g\frac{\Delta z \Delta T}{T}$ which is Eq.(4.9) with α replaced by T^{-1}. The vertical heat transport by a population of cumulus clouds is then given by Eq.(4.10) with α replaced by T^{-1}. This fairly crude model of convective vertical heat transport is a useful representation and yields realistic values. If convection carries heat at a rate of $200\mathrm{W\,m^{-2}}$ from the surface up to 1 km, Eq.(4.10) predicts $\Delta T \simeq 0.1\,\mathrm{K}$ and $w \simeq 1.5\,\mathrm{m\,s^{-1}}$, roughly in accord with what is observed.

Cumulonimbus convection

Suppose we had imagined that the Cu cloud discussed above had a vertical scale of 10 km rather than the 1 km assumed. We will see in Chapter 5 that the wind at a height of 10 km is some $20 - 30\,\mathrm{m\,s^{-1}}$ faster than at cloud base (see Fig.5.20) and so the cumulus cloud would be ripped apart. However, Cb storms move at the same speed as some middle-level wind. Fig.4.25 shows the flow relative to a cumulonimbus storm moving along with the wind at mid-levels. It overtakes the potentially warm air near the surface and so, relative to the storm, this air flows strongly toward the storm, ascends in the cloud and is eventually expelled as an anvil in a shallow, fast-moving sheet containing ice crystals. Release of latent heat in condensation (and associated heavy rain) in the updraft creates positive buoyancy and vertical acceleration, powering the motion. A region of low pressure is created at the surface just ahead of the storm, 'sucking' low level flow into it. At the same time upper-middle level air approaches the storm from behind, is cooled by evaporation from the rain falling into it, and brought down to the ground where it creates a region of high pressure as it decelerates. The 'squall front' is a stagnation point relative to the storm which moves roughly at the speed of the storm.

In contrast to a cumulus cloud, there is hardly any mixing in a cumulonimbus cloud because the flow is so streamlined. Consequently nearly all the potential energy released goes into kinetic energy of the updraft. Hence $\frac{1}{2}w^2 \sim g\frac{\Delta T}{T}\Delta z$ which yields $w \sim 25\,\mathrm{m\,s^{-1}}$ if $\Delta T \sim 1\,\mathrm{K}$ and $\Delta z \sim 10\,\mathrm{km}$, not

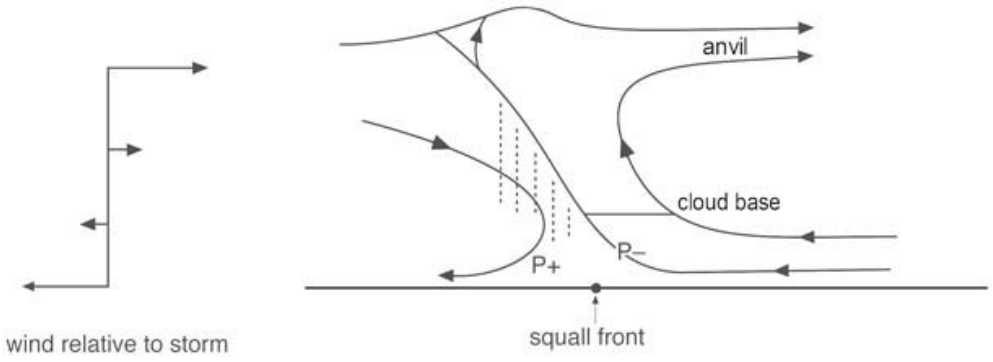

Figure 4.25: The pattern of flow relative to a cumulonimbus storm moving along with a middle-level wind. Ahead of the storm, air is sucked in ($p-$), ascends and is expelled in the anvil. Upper-middle level air approaches the storm from behind and is brought down to the ground ($p+$). The 'squall front' is a stagnation point relative to the storm which moves roughly at the speed of the storm. Heavy rain is represented by the vertical dotted lines in the updraught. Modified from Green, 1999.

untypical of the observations. Updrafts of this magnitude are strong enough, for example, to suspend hailstones until they grow to a large size.

4.6.2 Where does convection occur?

The short answer to this question is, in fact, almost everywhere. However, deep convection is common in some places and rare in others. In general, tropical rainfall is associated with deep convection, which is most common in the three equatorial regions where rainfall is most intense (Indonesia and the western equatorial Pacific Ocean, Amazonia, and equatorial Africa). Over the desert regions of the subtropics, it is uncommon. The contrast between these two areas is shown in the distribution of outgoing longwave radiation (OLR) in Fig.4.26.

OLR is the total radiative flux in the terrestrial wavelengths, measured by downward-looking satellite instruments. As discussed in Chapter 2, if we can think of this flux as emanating from a single layer in the atmosphere, then we can deduce the temperature of that layer [assuming blackbody radiation, Eq.(2.2)]. So OLR is a measure of the temperature of the emitting

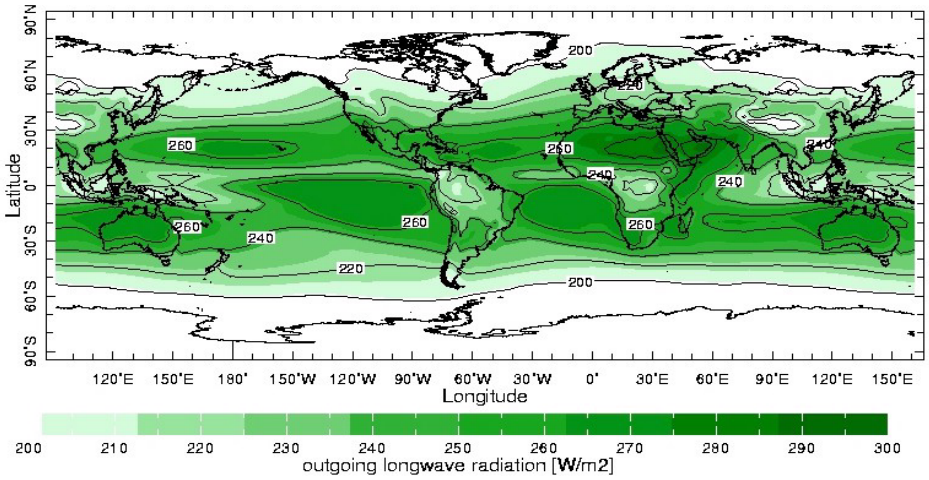

Figure 4.26: Outgoing longwave radiation (OLR: contour interval 20 Wm^{-2}) averaged over the year. Note the high values over the subtropics and low values over the three wet regions on the equator: Indonesia, Amazonia and equatorial Africa.

region. Note that the polar regions in Fig.4.26 have low OLR: this is not very surprising, since these regions are cold. The OLR is also low, however, over the three equatorial regions mentioned above. The radiation cannot be coming from the surface there, since the surface is warm; it must be (and is) coming from high altitudes ($10 - 15\,\mathrm{km}$, in fact), where the temperature is low, even in the tropics. As shown in Fig.4.27, this happens because the radiation is coming from the tops of deep convective clouds: the low OLR is indicative of deep convection. Note that in the subtropical regions, especially over the deserts and cooler parts of the ocean, OLR is high; these regions are relatively dry and cloud-free, and the radiation is coming from the warm surface.

Convection requires a warm surface *relative to the environmental air aloft.* This can be achieved by warming the surface by, for example, solar heating, leading to afternoon convection, especially in summer and, most of all, in the tropics where deep convection is very common. However, convection can also be achieved by cooling the air aloft. The latter occurs when winds bring cold air across a warm surface; for example, thunderstorms in middle

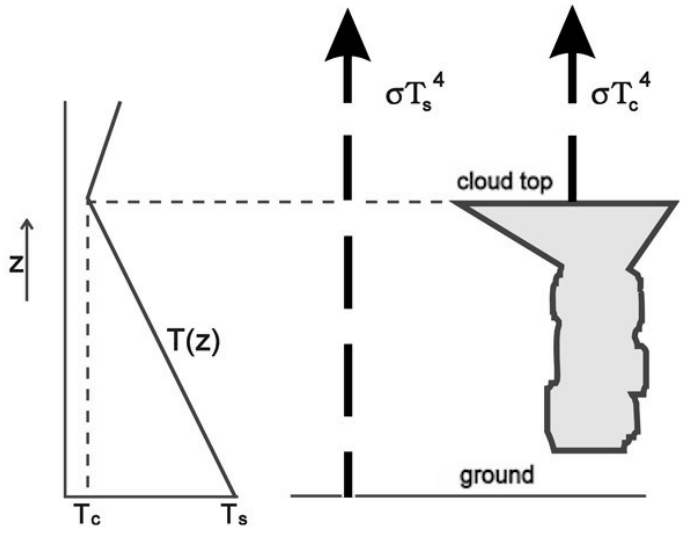

Figure 4.27: Schematic of IR radiation from the ground (at temperature $T_s \simeq 300\,\mathrm{K}$ in the tropics) and from the tops of deep convective clouds (at temperature $T_c \simeq 220\,\mathrm{K}$).

latitudes are frequently associated with the passage of cold fronts. In middle latitudes, shallow convection is frequent (and is usually visible as cumulus clouds). Deep convection (always associated with heavy rain and often with thunderstorms) is intermittent.

4.7 Radiative-convective equilibrium

As we saw in Section 3.1.2, the thermal structure expected on the basis of radiative forcing alone has a temperature discontinuity at the ground, as illustrated in Fig.3.4: the radiative equilibrium temperature of the ground is considerably warmer than that of the air above. This profile is unstable and convection will occur. Convective motions will transport heat upward from the surface; when the air parcels mix with the environment (as they will) they increase the environmental temperature until the environment itself approaches a state of neutrality which, in the moist tropical atmosphere, is one of constant moist potential temperature. The tropical troposphere is in-

deed observed to be close to neutral for moist convection (cf. Fig.4.9) where convection reaches up to the tropopause at height z_T. The whole tropical troposphere is in a state of *radiative-convective equilibrium*, with a convectively determined state below the tropopause and a radiative equilibrium state above, as sketched in Fig.3.4.

How the temperature structure of the tropics is conveyed into middle latitudes is less certain. It seems unlikely that local convection is the primary control of the vertical temperature structure in middle latitudes. Here transport by larger scale systems plays an important role. In Chapter 8 we will discuss the role of mid-latitude weather systems in transporting heat, both vertically and horizontally.

4.8 Further reading

The reader is referred to Holton (2004) and especially to Wallace and Hobbs (2006) for a more detailed discussion of atmospheric thermodynamics, where many of the more exotic thermodynamic variables are defined and discussed. Emanuel (1994) gives a very thorough and advanced treatment of atmospheric convection.

4.9 Problems

1. Show that the buoyancy frequency, Eq.(4.22), may be written in terms of the environmental temperature profile thus:

$$N^2 = \frac{g}{T_E}\left(\frac{dT_E}{dz} + \Gamma_d\right)$$

   where Γ_d is the dry adiabatic lapse rate.

2. From the temperature (T) profile shown in Fig.4.9:

   (a) estimate the tropospheric lapse rate and compare to the dry adiabatic lapse rate.

   (b) estimate the pressure scale height RT_0/g, where T_o is the mean temperature over the 700 mbar to 300 mbar layer.

   (c) estimate the period of buoyancy oscillations in mid-troposphere.

3. Consider the laboratory convection experiment described in Section 4.2.4. The thermodynamic equation (horizontally averaged over the tank) can be written:

$$\rho c_p \frac{dT}{dt} = \frac{\mathcal{H}}{h} \tag{4.31}$$

where h is the depth of the convection layer — see Fig.4.28 — $\mathcal{H}$ is the (constant) heat flux coming in at the bottom from the heating pad, ρ is the density, c_p is the specific heat, t is time and T is temperature.

We observe that the temperature in the convection layer is almost homogeneous and 'joins on' to the linear stratification into which the convection is burrowing, as sketched in Fig.4.28. Show that if this is the case, Eq.(4.31) can be written thus:

$$\frac{\rho c_p \overline{T_z}}{2} \frac{d}{dt} h^2 = \mathcal{H}$$

where $\overline{T}$ is the initial temperature profile in the tank prior to the onset of convection and $\overline{T_z} = \frac{d\overline{T}}{dz}$ is the initial stratification, assumed here to be constant.

   (a) Solve the above equation, show that the depth and temperature of the convecting layer increases like $\sqrt{t}$, and sketch the form the solution.

   (b) Is your solution consistent with the plot of the observed temperature evolution from the laboratory experiment shown in Fig.4.8?

   (c) How would T have varied with time if initially the water in the tank had been of uniform temperature (i.e. was unstratified)? You may assume that the water remains well mixed at all times and so is of uniform temperature.

4. Consider an atmospheric temperature profile at dawn with a temperature discontinuity (inversion) at 1km, and a tropopause at 11km, such that

$$T(z) = \begin{cases} 10\,^\circ\mathrm{C}, & z < 1\,\mathrm{km} \\ [15 - 8\,(z-1)]\ ^\circ\mathrm{C} & 1 < z < 11\,\mathrm{km} \\ -65\,^\circ\mathrm{C} & z > 11\,\mathrm{km} \end{cases}$$

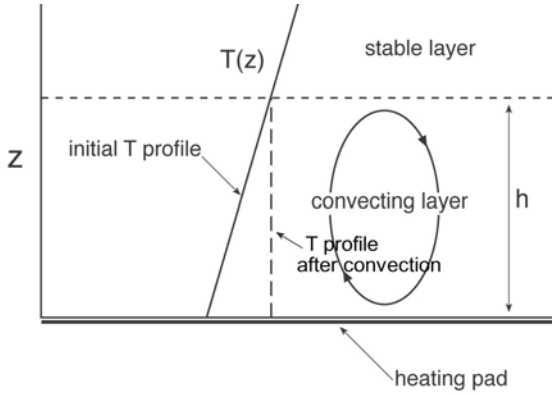

Figure 4.28: Schematic of temperature profiles before and after convection in the laboratory experiment GFD Lab II. The initial T profile, increasing linearly with height, is returned to the neutral state, one of uniform temperarture, by convection.

(where here z is expressed in km). Following sunrise at 6 a.m. until 1 p.m., the surface temperature steadily increases from its initial value of 10 °C at a rate of 3 °C per hour. Assuming that convection penetrates to the level at which air parcels originating at the surface and rising without mixing, attain neutral buoyancy, describe the evolution during this time of convection

(a) if the surface air is completely dry

(b) if the surface air is saturated.

You may assume the dry/wet adiabatic lapse rate is $10\,\mathrm{K\,km^{-1}}/7\,\mathrm{K\,km^{-1}}$ respectively.

5. For a perfect gas undergoing changes dT in temperature and dV in specific volume, the change ds in specific entropy, s, is given by

$$T\,ds = c_v dT + p\,dV\ .$$

(a) Hence, for unsaturated air, show that potential temperature θ

$$\theta = T\left(\frac{p_0}{p}\right)^{\kappa},$$

is a measure of specific entropy; specifically, that

$$s = c_p \ln\theta + \text{constant} \ ,$$

where c_v and c_p are specific heats at constant volume and constant pressure, respectively.

(b) Show that if the environmental lapse rate is dry adiabatic — Eq.(4.14) — then it has constant potential temperature.

6. Investigate under what conditions we may approximate $\frac{L}{c_p T} dq_*$ by $d\left(\frac{Lq_*}{c_p T}\right)$ in the derivation of Eq.(4.30). Is this a good approximation in typical atmospheric conditions?

7. Assume the atmosphere is in hydrostatic balance and isothermal with temperature 280 K. Determine the potential temperature at altitudes of 5 km, 10 km, and 20 km above the surface. If an air parcel were moved adiabatically from 10 km to 5 km, what would its temperature be on arrival?

8. Somewhere (in a galaxy far, far away) there is a planet whose atmosphere is just like that of the Earth in all respects but one — it contains no moisture. The planet's troposphere is maintained by convection to be neutrally stable to vertical displacements. Its stratosphere is in radiative equilibrium, at a uniform temperature −80 °C, and temperature is continuous across the tropopause. If the surface pressure is 1000 mbar, and equatorial surface temperature is 32 °C, what is the pressure at the equatorial tropopause?

9. Compare the dry-adiabatic lapse rate on Jupiter with that of Earth given that the gravitational acceleration on Jupiter is $26\,\mathrm{m\,s^{-2}}$ and its atmosphere is composed almost entirely of hydrogen and therefore has a different value of c_p.

10. In Section 3.3 we showed that the pressure of an isothermal atmosphere varies exponentially with height. Consider now an atmosphere with uniform *potential temperature*. Find how pressure varies with height, and show in particular that such an atmosphere has a discrete top (where $p \to 0$) at altitude $RT_o/(\kappa g)$, where R, κ, and g have their usual meanings, and T_o is the temperature at 1000 mbar pressure.

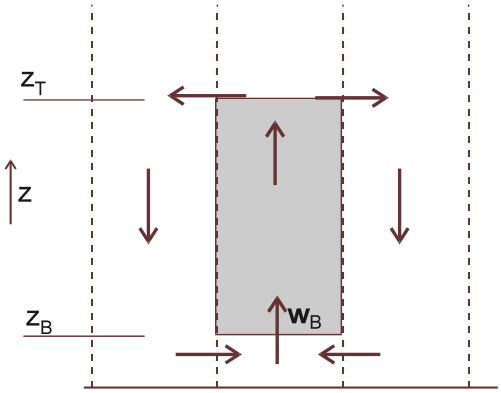

Figure 4.29: Air rises in the center of a convective cell with speed w_B at cloud base. Cloud is represented by shading; condensation occurs at altitude z_B and extends up to z_T at which point the air diverges and descends adiabatically in the downdraft region.

11. Consider the convective circulation shown in Fig.4.29. Air rises in the center of the system; condensation occurs at altitude $z_B = 1\,\text{km}$ ($p_B = 880\,\text{mbar}$), and the convective cell (cloud is shown by the shading) extends up to $z_T = 9\,\text{km}$ ($p_T = 330\,\text{mbar}$), at which point the air diverges and descends adiabatically in the downdraft region. The temperature at the condensation level, T_B, is $20\,^\circ\text{C}$. Assume no entrainment and that all condensate falls out immediately as rain.

    (a) Determine the specific humidity at an altitude of 3 km within the cloud.

    (b) The upward flux of air, per unit horizontal area, through the cloud at any level z is $w(z)\rho(z)$, where ρ is the density of dry air and w the vertical velocity. Mass balance requires that this flux be independent of height within the cloud. Consider the net upward flux of water vapor within the cloud and hence show that the rainfall rate below the cloud (in units of mass per unit area per unit time) is $w_B\rho_B\left[q_{*B} - q_{*T}\right]$, where the subscripts "$_B$" and "$_T$" denote the values at cloud base and cloud top, respectively. If $w_B = 5\,\text{cm s}^{-1}$, and $\rho_B = 1.0\,\text{kg m}^{-3}$, determine the rainfall rate in cm per day.

12. Observations show that, over the Sahara, air continuously subsides (hence the Saharan climate). Consider an air parcel subsiding in this region, where the environmental temperature T_e decreases with altitude at the constant rate of $7\,\mathrm{K\ km^{-1}}$.

    (a) Suppose the air parcel leaves height z with the environmental temperature. Assuming the displacement to be adiabatic, show that, after a time δt, the parcel is warmer than its environment by an amount $w\Lambda_e\delta t$, where w is the subsidence velocity and

    $$\Lambda_e = \frac{dT_e}{dz} + \frac{g}{c_p}\ ,$$

    where c_p is the specific heat at constant pressure.

    (b) Suppose now that the displacement is not adiabatic, but that the parcel cools radiatively at such a rate that its temperature is *always the same as* its environment (so the circulation is in equilibrium). Show that the radiative rate of energy loss per unit volume must be $\rho c_p w\Lambda_e$, and hence that the net radiative loss to space, per unit horizontal area, must be

    $$\int_0^\infty \rho c_p w\Lambda_e\ dz\ = \frac{c_p}{g}\int_0^{p_s} w\Lambda_e\ dp\ ,$$

    where p_s is surface pressure and ρ is the air density.

    (c) Radiative measurements show that, over the Sahara, energy is being lost to space at a net, annually-averaged rate of $20\mathrm{W\,m^{-2}}$. Estimate the vertically-averaged (and annually-averaged) subsidence velocity.